

# Effects of the deposition temperature on the resistivity of copper films produced by low-pressure metal–organic chemical vapour deposition on a TiN barrier layer

S. S. YOON, J. S. MIN, J. S. CHUN

*Department of Electronic Materials Engineering, Korea Advanced Institute of Science and Technology, 373-1, Kusung-dong, Yusung-gu, Taejon, 305-701, Korea*

Copper was deposited on to TiN by low-pressure metal–organic chemical vapour deposition, using hexafluoroacetylacetonate–Cu<sup>+1</sup>–trimethylvinylsilane (hfacCu(I)TMVS) and argon carrier gas. The resistivity of the deposited copper films was investigated by observing the effects of the deposition temperature on the composition, microstructure and surface morphology of the copper films. The resistivity of the copper films decreases as the deposition temperature decreases. The copper films deposited at high temperatures, tend to contain the pores and or/ channels as well as carbon and oxygen, which results in the increase of the resistivity of the deposited films. The pores and/or channels come from the island-like growth of the copper films, while carbon and oxygen are due to the concurrent thermal decomposition of hfac during the disproportionation reaction between hfacCu(I) molecules.

## 1. Introduction

There is great technological growth in the area of integrated circuit (IC) device fabrication in the semiconductor industry, which has led to continually shrinking device feature size [1]. The width and thickness of the interconnection lines continue to decrease, while the aspect ratio of the contacts/vias continues to increase. However, these require more serious consideration of the metallization process to improve the RC time delay and the reliability problem of the interconnection lines [2–5]. Although aluminium-based alloy deposited by sputtering is still being used for the metallization process, it has fundamental problems that must be solved urgently as the minimum feature size goes down to the sub-half micrometer: the RC time delay problem due to the high resistivity (3–4  $\mu\Omega$  cm) of aluminium-based alloy [6, 7], and the reliability problems associated with the nonconformal deposition property of the sputtering method itself [7–8].

Chemical vapour deposition of copper has been widely considered as a possible solution because of the low bulk resistivity (1.67  $m\mu\Omega$  cm) of copper as well as its conformal deposition property [9]. Among the development of such an approach, exclusively, low-pressure metal–organic chemical vapour deposition (LPMOCVD) of copper has been intensively studied for its ability to produce copper films at reduced temperatures with high degrees of perfection and low resistivity [10–14].

However, relatively little work has been performed on the deposition of copper films on the barrier layers which must be used for copper metallization in ultra-large-scale integration (ULSI) circuits to keep copper from diffusing into silicon or silicon oxide [15]. Furthermore, only limited work has been undertaken to examine the effects of film characteristics on the resistivity of copper films on barrier layers.

In this study, copper films were deposited with hexafluoroacetylacetonate–Cu<sup>+1</sup>–trimethylvinylsilane (hfacCu(I)TMVS) and argon carrier gas by LPMOCVD on to a TiN layer, one of the potential candidates for barrier layers. By examining the film characteristics at various deposition temperatures, such as composition, microstructure and surface morphology, the effects of the deposition temperature on the resistivity of copper films were investigated.

## 2. Experimental procedure

### 2.1. LPMOCVD apparatus

Fig. 1 shows a schematic diagram of the LPMOCVD apparatus for deposition of the copper films in this study. It can be divided into four parts: the gas feeding part, the precursor container, the reaction chamber and the vacuum system. The gas feeding part, which transports hfacCu(I) TMVS and argon carrier gas to the reaction chamber, consists of gas filters, air-operated bellows valves, a mass flow controller (MFC), a fine metering bellows valve and 1/4 in ( $\sim 6$  mm) 316

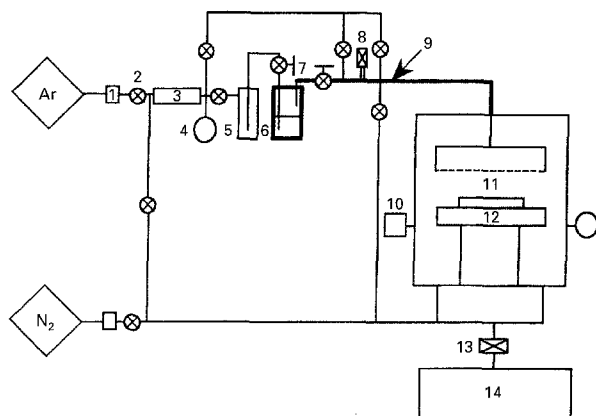


Figure 1 Schematic drawing of the LPMOCVD apparatus for deposition of the copper films. 1, Filter; 2, air-operated bellows valve; 3, mass flow controller; 4, Bourdon gauge; 5, empty trap; 6, precursor container; 7, manual bellows valve; 8, fine metering bellows valve; 9, heating part; 10, capacitance manometer; 11, reaction chamber; 12, susceptor; 13, butterfly valve; 14, pumping system.

stainless steel tube. In particular, the part between the precursor container and the reaction chamber is maintained at 60 °C to prevent condensation of hfacCu(I) TMVS during the delivery. The precursor container has been designed to be bubbled by argon carrier gas to increase the rate of vaporization of hfacCu(I) TMVS and is heated homogeneously at 50 °C through the silicon oil bath during the deposition. The reaction chamber, made of 316 stainless steel, is a cold-wall type and the gases are showered downwards to the substrate. The substrate is heated by the resistant heater and the substrate temperature is measured by a K-type thermocouple which is directly in contact with the substrate. The vacuum system consists of the capacitance manometer (Baratron pressure gauge, MKS Co.) and the mechanical rotary pump.

## 2.2. Deposition conditions

The TiN substrates, size 2 × 2 cm<sup>2</sup>, were prepared by sputtering on the p-type (100) silicon single crystals. The thickness of the TiN layer was 70 nm and its resistivity ranged from 150–200 μΩ cm. The copper films were deposited at a fixed deposition pressure (1 torr; ~ 133.322 Pa) and the fixed flow rate of hfacCu(I)TMVS. The flow rate of hfacCu(I)TMVS was fixed through the bubbling Equation 1 [16], by maintaining a constant temperature (50 °C) and pressure (40 torr) of the precursor container and the constant flow rate (200 standard cm<sup>3</sup> min<sup>-1</sup>) of argon carrier gas.

$$F_{\text{hfacCu(I)TMVS}} = P_v \times F_{\text{Ar}} / (P_b - P_v) \quad (1)$$

where  $F_{\text{hfacCu(I)TMVS}}$  is the flow rate of hfacCu(I)TMVS,  $F_{\text{Ar}}$  is the flow rate of argon carrier gas,  $P_b$  is the pressure of the precursor container, and  $P_v$  is the vapour pressure of hfacCu(I)TMVS, which depends on the temperature of the precursor container. Other deposition parameters being fixed, the deposition temperatures were varied from 145–405 °C.

## 2.3. Characterization methods

The thickness of the deposited copper films was measured using a surface profilometer (Alpha-Step 2000, Tencor Instrument Co.) and confirmed by cross-sectional scanning electron microscope (X-SEM). To form a step in the copper layer, photoresist (P/R) was patterned on the copper films through the photolithography process, then the copper layer was selectively etched in a dilute nitric acid solution (DI:HNO<sub>3</sub> = 10:1) and the patterned P/R was finally removed by acetone. The resistivity of the copper films was measured using a linear four-point probe (C4S-44 model, Alessi Co.) method. The composition of the deposited films was investigated by Auger electron spectroscopy (AES), after sputtering for 7 min by an argon ion beam in the AES chamber to remove the surface contaminants. The energy and the current of the primary electron beam were adjusted, respectively, to 5 keV and 1 μA. A scanning electron microscope (SEM) was used to observe the surface morphology and X-ray diffraction (XRD) was carried out to examine the film structure. The voltage and the current of the X-ray tube were set, respectively, at 40 kV and 120 mA, and the measurements were performed using CuK<sub>α</sub> with a scan speed of 4° min<sup>-1</sup> in the 20°–80° (2θ) region. The microstructure of the deposited films was investigated by transmission electron microscopy (TEM) with an acceleration voltage of 200 kV. The TEM specimens were prepared by mechanical polishing from the rearside of silicon, followed by argon-ion beam milling to a thickness of less than 100 nm. Also, the reflectance of the deposited copper films was measured using a nanospectrometer; this measurement was used in deriving the surface roughness.

## 3. Results and discussion

Fig. 2 shows the variations of the resistivity of the copper films with 600 nm thickness on TiN, as a

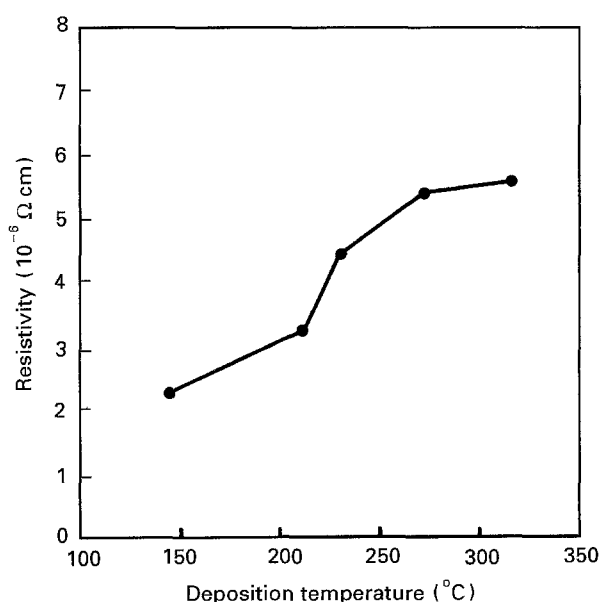


Figure 2 Resistivity of the copper films as a function of the deposition temperature: deposition thickness, 600 nm; deposition pressure, 1 torr; argon flow rate, 200 standard cm<sup>3</sup> min<sup>-1</sup>; pressure of precursor container, 40 torr; temperature of precursor container, 50 °C.

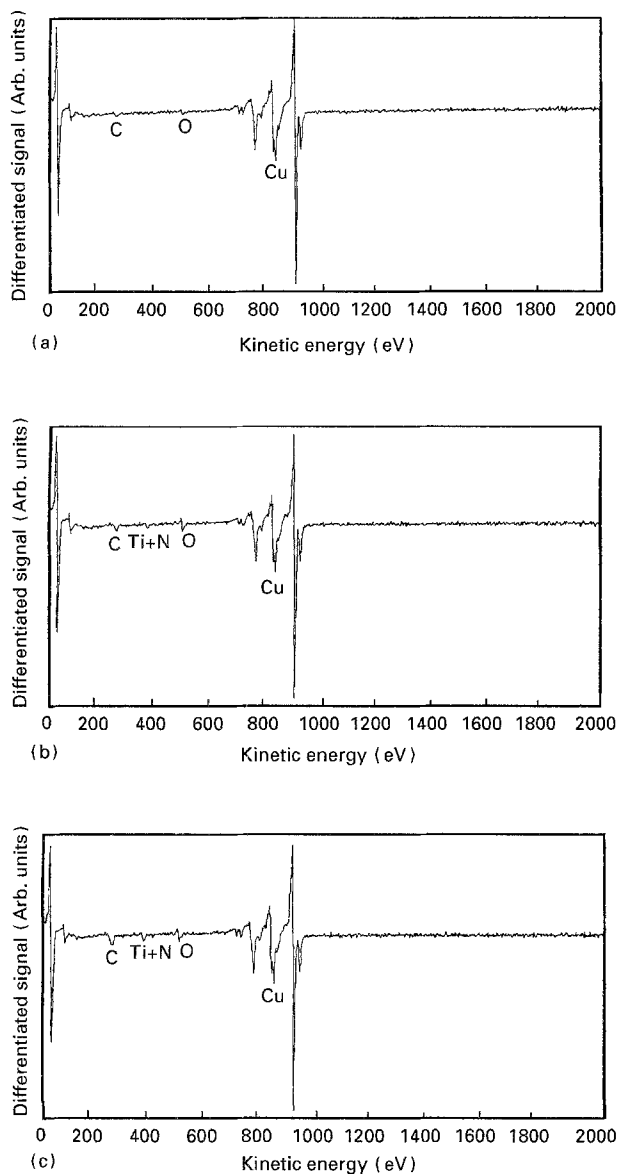


Figure 3 Differentiated AES spectra of the copper films, after sputtering the surface contaminants. Deposition temperature; (a) 145 °C, (b) 231 °C, (c) 405 °C.

function of the deposition temperature. As the deposition temperature increases, the resistivity of the copper films also increases. This is similar to the results given by Norman *et al.* [17] who deposited the copper films on SiO<sub>2</sub>.

Fig. 3 shows the AES spectra from the copper films at various deposition temperatures. While the content of impurities, such as carbon and oxygen, is of the order of the detection limit ( $\sim 1$  at%) in the case of 145 °C, it increases as the deposition temperature increases. However, regardless of the deposition temperatures, there are no other impurity peaks, such as silicon peaks (at 92 eV from *LMM* transition and at 1619 eV from *KLL* transition). It indicates that the separation rate of TMVS(Si(CH<sub>3</sub>)<sub>3</sub>CH<sub>2</sub>CH) from the adsorbed hfacCu(I)TMVS(CF<sub>3</sub>COCHCOCF<sub>3</sub>-Cu<sup>+1</sup>(I)Si(CH<sub>3</sub>)<sub>3</sub>CH<sub>2</sub>CH) and the desorption rate of TMVS from the leading surface of the deposit, are very rapid in our deposition conditions. Therefore, it can be inferred that carbon and oxygen in the copper films deposited at high temperatures have originated

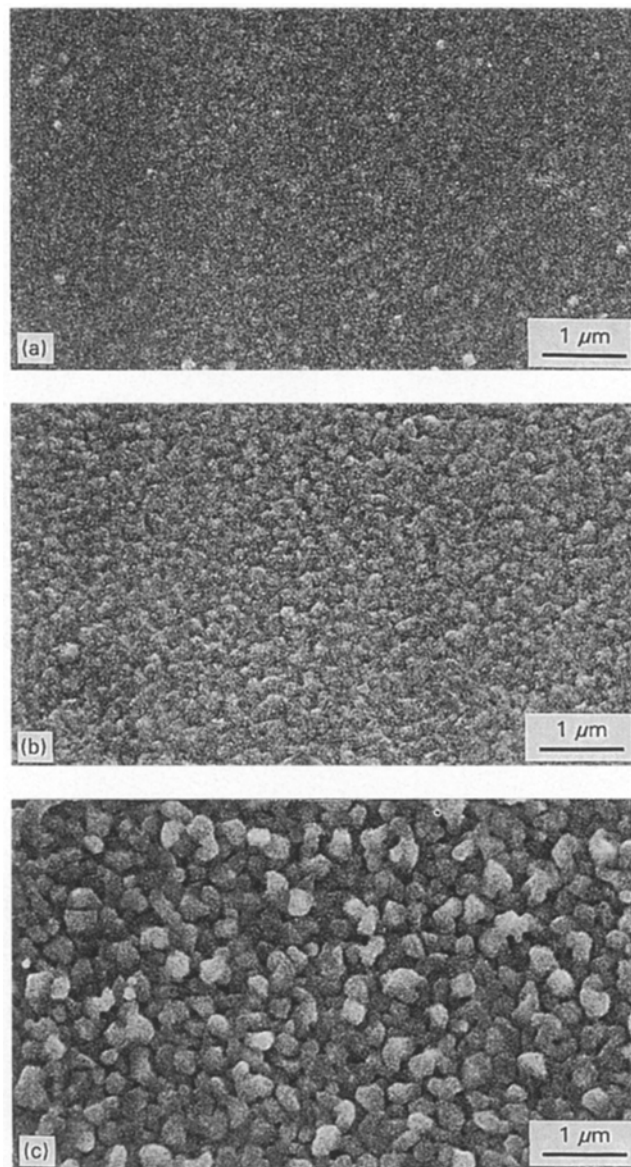


Figure 4 SEM images for the surface morphology of the copper films. Deposition temperature; (a) 145 °C, (b) 188 °C, (c) 231 °C.

from the thermal decomposition of hfac(CF<sub>3</sub>COCHCOCF<sub>3</sub>), the constituent of the remaining hfacCu(I). Donnelly and Gross [18], who studied the thermal decomposition reaction of hfacCu(I)TMVS in ultra-high vacuum ( $1 \times 10^{-9}$ – $2 \times 10^{-10}$  torr) conditions, reported a similar tendency that hfacCu(I)TMVS adsorbed on the TiN surface changes very rapidly into hfacCu(I) and, under some surface conditions, the thermal decomposition reaction of hfacCu(I) can occur concurrently with the disproportionation reaction between hfacCu(I) molecules. So, under the present deposition conditions (1 torr), it is also thought that paths of copper deposition include the thermal decomposition reaction as well as the disproportionation reaction, and that the increase of the deposition temperature causes the increase in the ratio of the decomposition reaction to the disproportionation reaction. The increased content of carbon and oxygen is a factor which results in the increase of the resistivity of the deposited copper films in our study.

Fig. 4 shows the surface morphology of the copper films at various deposition temperatures. As the

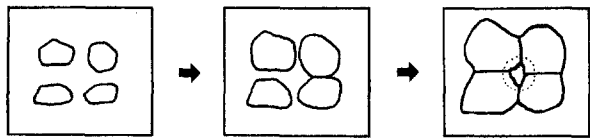


Figure 5 Model showing how pores and/or channels are formed in the films.

deposition temperature increases, the continuous surface of the copper films gradually changes into the island-like surface which has the macroscopic boundaries between the neighbouring sites. Generally, this island-like three-dimensional morphology is formed under circumstances when the growth of nuclei can occur neither by the surface diffusion of the atoms

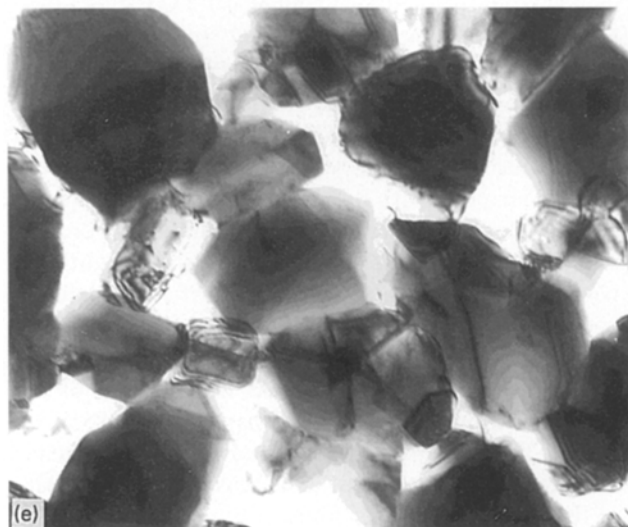
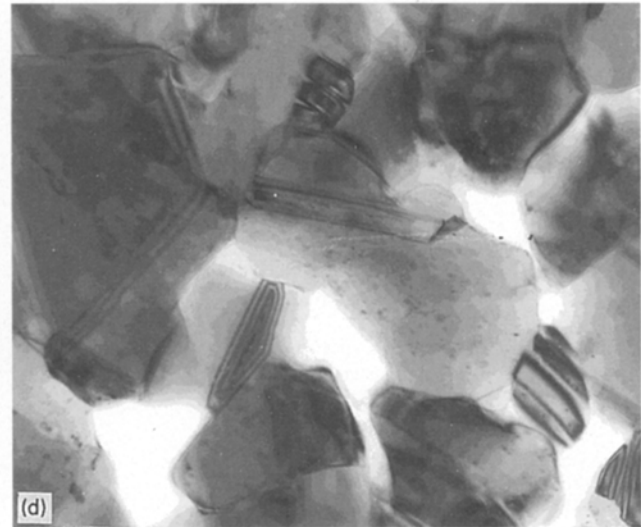
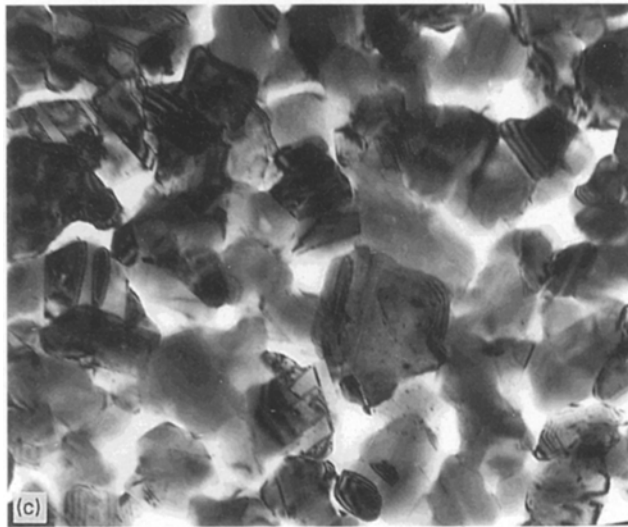
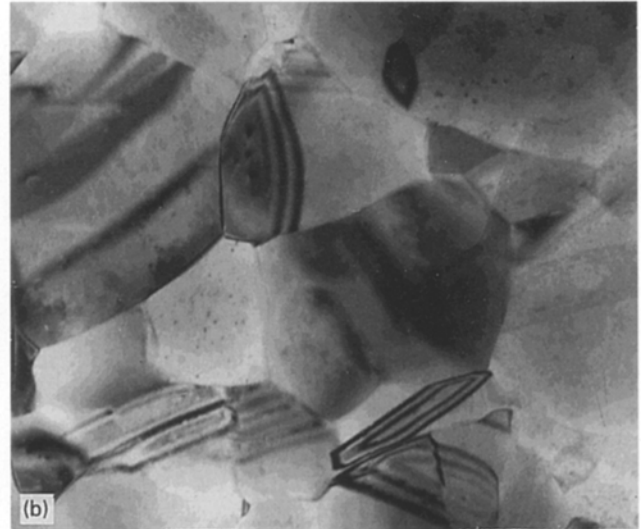
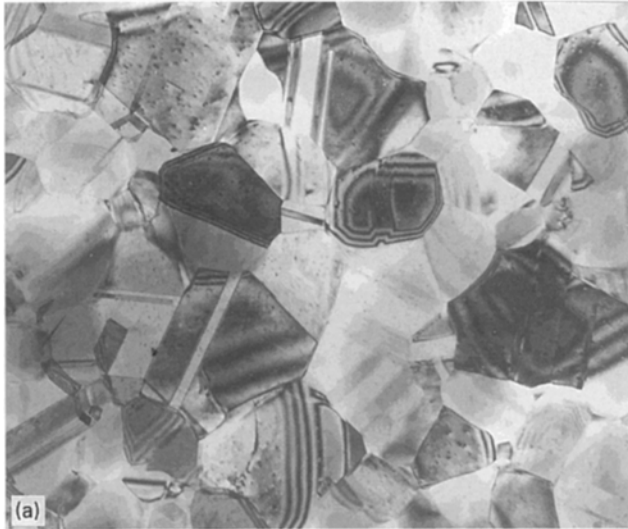


Figure 6 TEM images for the microstructure of the copper films. Deposition temperature; (a, b) 145 °C, (c, d) 231 °C, (e, f) 317 °C.

which have already been deposited elsewhere, nor by the deposition from the reactants which have arrived next to the nuclei through the surface diffusion. Under such circumstances, the nuclei prefer growth by the deposition from the reactants which have adsorbed directly on the nuclei, which results in the island-like three-dimensional morphology. Therefore, under the present deposition conditions, it is thought that the increase of the deposition temperature enhances *relatively* the rate of the deposition of copper from hfacCu(I)TMVS which has adsorbed directly onto the nuclei, rather than the rate of the surface diffusion of the deposited copper atom or adsorbed hfacCu(I)-TMVS. When the nuclei grow like the islands, the disconnected parts are formed during the coalescence stage, as shown in Fig. 5. And, if the films grow rapidly without sufficient surface diffusion, pores and/or channels can remain within the films [19].

Fig. 6 shows the TEM images of the copper films at various deposition temperatures. As shown in Fig. 6a, c and e, the disconnectivity appeared to be seriously affected as the deposition temperature increases. This is very consistent with the results of AES spectra, as shown previously in Fig. 3b and c. In Fig. 3b and c, there are Ti + N peaks originated from the TiN substrate, which indicates that the microvoids, such as pores and/or channels, have been incorporated in the copper films deposited at high temperatures. However, there is no marked difference in the defects within the grain in Fig. 6b, d and e. The XRD results of the copper films (Fig. 7) show that regardless of the deposition temperatures, all of the deposited copper films have the structure of a fcc Bravais lattice. Therefore, in the present study, the major effect of the deposition temperature on the structure of the copper films is to increase the tendency for the incorporation of the pores and/or channels into the films, while the other properties, such as the lattice structure and the defect density within the grain, are little influenced by the deposition temperature. As a matter of course, those pores and/or channels, incorporated at the high deposition temperatures, act greatly on the increase of the resistivity by blocking the travelling electrons. Conclusively, a high deposition temperature is another cause of the increase in the resistivity in the copper films, by inducing the island-like structure which contains the pores and/or channels.

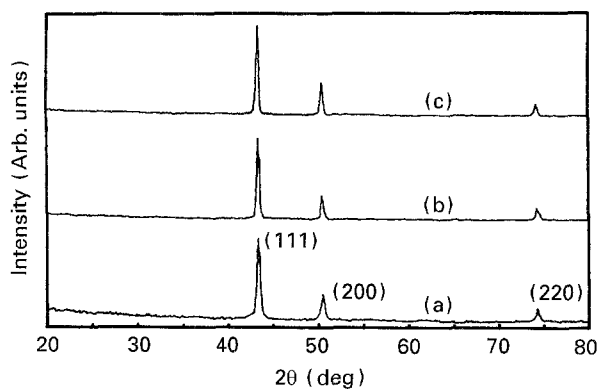


Figure 7 XRD results of the copper films. Deposition temperature; (a) 145 °C, (b) 231 °C, (c) 405 °C.

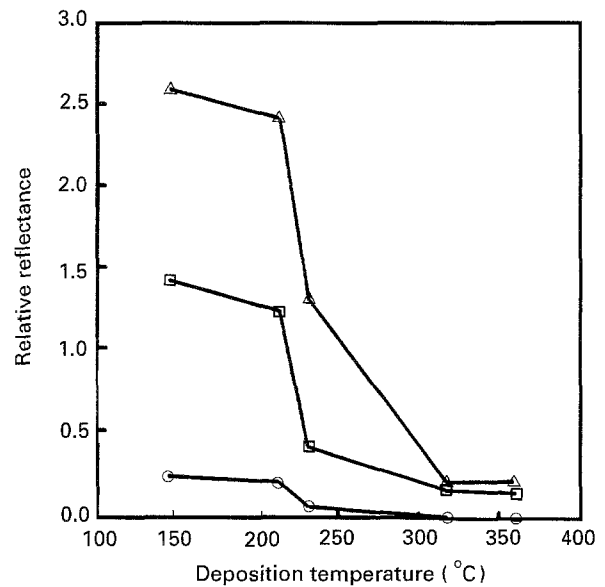


Figure 8 Relative reflectances of the copper films at (○) 400 nm, (□) 600 nm and (△) 800 nm as a function of the deposition temperature.

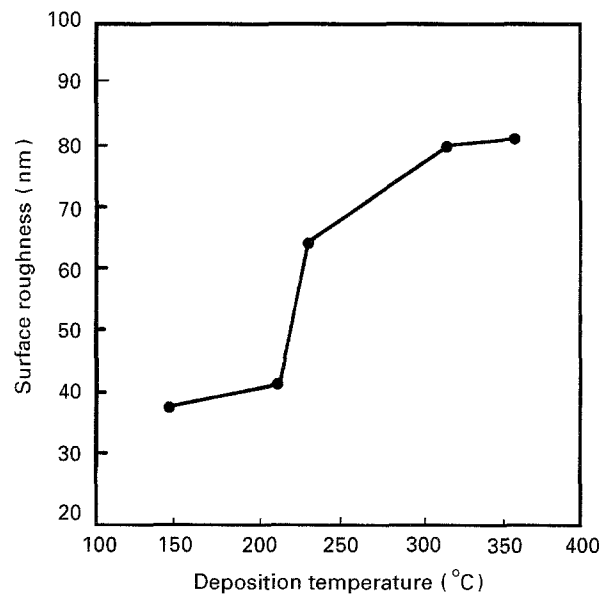


Figure 9 Surface roughness of the copper films as a function of the deposition temperature.

Figs 8 and 9 show, respectively, the variations of the reflectance and the surface roughness of the copper films, as a function of the deposition temperature. The reflectance of the deposited copper surfaces,  $R_{Cu}$ , was measured relatively to the reflectance of the silicon standard wafer,  $R_{Si(s)}$ , and  $R_{Cu}/R_{Si(s)}$  was plotted as relative reflectance in Fig. 8. In Fig. 9, the surface roughness was expressed by the root-mean-square roughness,  $\sigma_0$  which had been derived from the values of  $R_{Cu}/R_{Si(s)}$ , and Table I [20–21], using Chiang *et al.*'s theory [22]. Following Chiang *et al.*'s theory, in the case of a rough copper surface, the relationship between the value of  $R_{Cu}$  and the root-mean-square roughness,  $\sigma_0$  is given in a first approximation by

$$R_{Cu}/R_{Cu(s)} (= R_{Cu}/R_{Si(s)} \times R_{Si(s)}/R_{Cu(s)}) \approx \exp[-(4\pi \cos \phi_0 \sigma_0 / \lambda)^2] \quad (2)$$

TABLE I Values of the reflectances for the silicon and the copper standard surfaces at various wavelengths

	Wavelength (nm)		
	400	600	800
$R_{\text{Si(s)}}$	0.48	0.35	0.33
$R_{\text{Cu(s)}}$	0.46	0.94	0.98

where  $R_{\text{Cu(s)}}$  is the reflectance of a smooth copper for a radiation of wavelength,  $\lambda$ , and incidence angle,  $\phi_0$ . This equation is valid for a statistically uniform copper surface of a roughness smaller than wavelength  $\lambda$ , consisting of facets of random shape and size, with Gaussian distribution of surface heights around the mean value. In Fig. 9, the surface roughness of the deposited copper films increases as the deposition temperature increases, which is well matched with the result of Fig. 4. As described before, the increase of the deposition temperature makes the copper films prefer the island-like structure which also causes the increases in the surface roughness of the copper films. In thin films, the rough surface prevents the conduction electrons from scattering specularly at the surface ([19] Ch. 13, p. 11), which results in the increase of the resistivity. In the present study, the increase of surface roughness with the deposition temperature is a further cause for the increase in the resistivity of the deposited copper films.

#### 4. Conclusion

The resistivity of copper films was investigated according to the deposition temperature when depositing the copper films on to TiN by LPMOCVD, using hfacCu(I)TMVS and argon carrier gas. The resistivity of the copper films decreased as the deposition temperature decreased, which resulted from the reduced content of impurities, such as carbon and oxygen, and from the change in the film structure, from the island-like structure to the continuous layer structure. It was also found that the island-like structure of the copper films deposited at high temperature contributed to the increase in the resistivity of the copper films in two respects. Firstly, it contributed to the increase of the resistivity by forming pores and/or channels within the copper films. Secondly, it contributed to the increase of the resistivity by increasing the surface roughness of the copper films.

#### 5. Acknowledgements

This work was supported by HEI (Hyundai Electronics Industries) Co. Ltd. We would like to acknowledge support from the Semiconductor Research and Development Laboratory of HEI Co., Ltd.

#### References

1. E. J. RYMASZEWSKY, *J. Electron. Mater.* **18** (1989) 217.
2. G. LARRABEE and P. CHATTERJEE, *Semicond. Int.* **14** (May, 1991) 84.
3. W. C. HOLTON, *SPIE* **1392** (1990) 27.
4. W. C. SHUMAY Jr. *Adv. Mater. Process.* **135** (1989) 43.
5. T. SEIDEL, in "Proceedings of the Sematech Fourth Annual Sematech Centers of Excellence (SCOE) Technology Transfer Meeting", (11 March, 1992) p. 121.
6. P. L. PAI, C. H. TING, C. CHIANG, C. S. WEI and D. B. FRASER, "Copper Interconnection for VLSI and Beyond", *MRS Symposia Proceedings VLSI V* 1990, p. 359.
7. ALAIN E, KALOYEROS and MICHAEL A. FURY, *MRS Bull.* June (1993) 22.
8. J. A. T. NORMAN, B. A. MURATONE, P. N. DYER, D. A. ROBERTS, A. K. HOCHBERG and L. H. DUBOIS, *J. Mater. Sci. Eng.* **B17** (1993) 87.
9. S. MURARKA, "Overview of Technology", in Conference Proceedings VLSI VI (1991) p. 179.
10. RAVI KUMAR, *Chem Mater.* **4** (1992) 577.
11. M. J. HAMPDEN-SMITH, T. T. KODAS, M. PAFFETT, J. D. FARR and H. K. SHIN, *ibid.* **2** (1990) 636.
12. A. JAIN, *Semicond. Int.* (June) **16** (1993) 128.
13. S. K. REYNOLDS, C. J. SMART, E. F. BARAN, T. H. BAUM, C. E. LARSON and P. J. BROCK, *Appl. Phys. Lett.* **59** (1991) 2332.
14. THOMAS H. BAUM and CARL E. LARSON, *J. Electrochem. Soc.* **140** (1993) 154.
15. J. D. McBRAYER, *ibid.* **133** (1986) 1262.
16. KLAUS K. SCHUEGRAF, "Handbook of Thin-Film Deposition Processes and Techniques" (Noyes, Park Ridge, NJ, 1988) p. 241.
17. J. A. T. NORMAN, B. A. MURATORE, P. N. DYER, D. A. ROBERTS and A. K. HOCHBERG, in "Proceedings of the International Very-Large-Scale Integration Multilevel Interconnection Conference, Santa Clara, CA, 11-12 June 1991 (IEEE, New York, 1991) p. 123.
18. V. M. DONNELLY and M. E. GROSS, *J. Vac. Sci. Technol. A* **11** (1993) 66.
19. LEON I. MAISSEL and REINHARD GLANG, "Handbook of Thin Film Technology" (McGraw-Hill, New York, 1983) Ch. 8, p. 35.
20. H. R. PHILIPP, *Phys. Rev.* **120** (37) (1960) 37.
21. D. DRISCOLL, "Handbook of Optics" (McGraw-Hill, New York, 1978).
22. K. L. CHIANG, C. J. DELL'OCA and F. N. SCHWETTMANN, *J. Electrochem. Soc.* **126** (1979) 2267.

Received 23 February  
and accepted 8 September 1994